

# Implementation of RSM and ANN Optimization Approach for Natural Deep Eutectic Solvents-Based Extraction of Bioactive Compounds from Orange Peel

Rachna Gupta, Anupama Singh,\* Prabhath K. Nema, Tapas Roy, Sanjay Kumar, and Avvaru Praveen Kumar\*



Cite This: *ACS Omega* 2024, 9, 34880–34892



Read Online

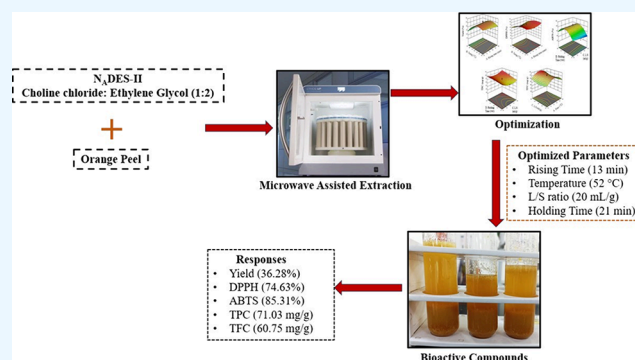
ACCESS |

Metrics & More

Article Recommendations

Supporting Information

**ABSTRACT:** The present investigation has focused on developing an eco-friendly method to extract bioactive compounds from orange peel using natural deep eutectic solvents (NADES). NADES-II composed of choline chloride (ChCl) and ethylene glycol (1:2) and 50% water shows the maximal extraction yield with higher antioxidant activity in terms of DPPH and ABTS scavenging activity with a high total phenolic content (TPC) and total flavonoid content (TFC). The microwave-assisted extraction (MAE) process was optimized using response surface methodology (RSM) and an artificial neural network (ANN). ANN showed a higher value of  $R^2$  and lower values of other statistical parameters when compared to RSM. The ideal extraction conditions were optimized as a 13 min rising time, 52 °C temperature, a 21 min holding time, and a 20 mL/g liquid-to-solid ratio. MAE was compared with the conventional heating-stirring extraction (HSE) method using the NADES-II solvent under optimum conditions. The results show that higher extraction yield and antioxidant capacities (DPPH and ABTS), TPC, and TFC can be obtained from orange peel using the MAE process compared to the HSE process. Overall, this study shows an optimization approach for the extraction of bioactive compounds from an orange peel using eco-friendly solvents and microwave technology. It also highlights the potential of this approach for valorizing orange peel waste.



## 1. INTRODUCTION

Around 115.5 million tonnes of oranges are produced worldwide each year, and their byproducts, which account for 50% of this total production, generate 3 million tonnes of garbage annually.<sup>1</sup> Peel (flavedo and albedo), pulp, and seeds all include several high-value-added compounds.<sup>2</sup> Bioactive compounds found in orange peel include essential oils, carbohydrate polymers, fermentable sugars, carotenoids, vitamins, flavonoids, and polyphenols.<sup>3</sup> Plant flavonoids perform a variety of biochemical functions and are important metabolites. These bioactive chemicals have historically been extracted using organic solvents; however, a majority of them are hazardous and cause environmental pollution when used. Most phytoconstituents have been thermally degraded by conventional extraction techniques that require longer extraction times. Traditional techniques suffer from these drawbacks.

Natural deep eutectic solvents ( $N_{A}DES_{s}$ ) are becoming more popular as an alternative to organic solvents.<sup>4</sup> According to Manurung and Siregar,<sup>5</sup> hydrogen bond acceptors ( $HB_{As}$ ) or donors ( $HB_{Ds}$ ) elements make up  $N_{A}DES_{s}$  originally presented a  $N_{A}DES_{s}$  that had urea ( $NH_{2}CONH_{2}$ ) as the  $HB_{D}$  and choline chloride ( $C_{3}H_{14}NO.Cl$ ) as the  $HB_{A}$ . Deep eutectic

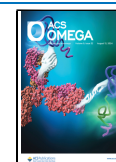
solvents, as opposed to organic solvents or ionic liquids (ILs), are employed as acceptable extraction media in the recovery of polyphenolic compounds from biomass waste because they are inexpensive, nontoxic, biodegradable, and easy to manufacture.<sup>7</sup>  $N_{A}DES_{s}$  are commonly used as solvents for the extraction of bioactive components from solid plant matrices.<sup>8</sup> Therefore, there is an increasing demand for innovative extraction techniques that use less solvent, take less time, and are more concerned with preventing contamination. According to Bubalo et al.,<sup>9</sup> MAE has advantages such as simple handling, automated approaches, and faster extraction times. The advantages of  $N_{A}DES_{s}$  include their nontoxicity, negligible vapor pressure, low flammability, environmental friendliness, and low waste generation. In contrast, employing microwaves

Received: May 11, 2024

Revised: July 22, 2024

Accepted: July 24, 2024

Published: August 2, 2024



can increase the effectiveness of extraction while consuming less time and solvent than conventional techniques.

MA-N<sub>A</sub>DESE (microwave-assisted natural deep eutectic solvent extraction) offers many potential advantages for recovering phenolic compounds from biomass waste. MA-N<sub>A</sub>DESE has grown dramatically in the past ten years, and for most applications, it has outperformed conventional extraction methods in every way. The MA-N<sub>A</sub>DESE of the plant matrix can be influenced by a variety of variables; including concentration of solvent, microwave power, irradiation time, temperature, and feed-to-solvent ratio.<sup>10</sup> These characteristics may impact the response (output).

Now these days, artificial neural networks (ANNs) have emerged as a strong alternative to response surface methodology (RSM) due to their ability to handle complex decision-making processes. ANNs are inspired by the human central nervous system, where a vast network of interconnected neurons computes information.<sup>11,12</sup> Modeling by ANNs has been extensively used in engineering applications to reduce processing time and achieve more accurate results, particularly when dealing with massive and complex data sets. A comparative study between MAE and heating-stirring extraction methods was also performed at optimized values to evaluate the effectiveness of MAE and heating-stirring extraction methods.

Therefore, the present investigation aims to optimize the natural deep eutectic solvent-based extraction of bioactive compounds from orange peel using RSM and results were ratified using ANN to achieve higher extraction yield of bioactive compounds as well as their TPC, TFC, DPPH, and ABTS potential.

## 2. MATERIALS AND METHODS

**2.1. Raw Materials and Chemicals.** Mature orange fruits were procured from the local market in Sonipat, Haryana (28.87° N, 77.13° E). The fruits were washed in tap water 2–3 times to remove the surface dust. Peels were removed manually and cleaned again in water. The washed peels were then dried for 10–12 h at 70 °C in an infrared dryer developed in the National Institute of Food Technology, Entrepreneurship and Management (NIFTEM-K) in Haryana, India. After drying, the dried peels were pulverized in a household grinder, and the fine powder (40 mesh) was kept in HDPE bags at room temperature for further analysis. The analytical-grade chemicals and standards utilized in this study were obtained from Hi-Media Pvt. Ltd., India.

**2.2. Preparation of N<sub>A</sub>DES<sub>s</sub>.** The modified method of Dai et al.<sup>13</sup> was used to create natural deep eutectic solvents. Choline chloride (ChCl) was chosen as HB<sub>A</sub> for the creation of N<sub>A</sub>DES<sub>s</sub>, while amides (urea), alcohols (ethylene glycol), carboxylic acids (lactic acid), and sugars (maltose) were chosen as the HB<sub>D</sub>s. HB<sub>A</sub> and HB<sub>D</sub>s were combined in a precise molar ratio (1:2) to create the N<sub>A</sub>DES<sub>s</sub> and the mixture was agitated at 60–80 °C in a water bath until a transparent liquid appeared.<sup>14</sup> Table 1 represents the codes of N<sub>A</sub>DES<sub>s</sub> along with the molar ratio and composition.

**2.3. Screening Using OFAT Approach.** The most important parameter for effective extraction i.e. types of N<sub>A</sub>DES, its concentration in water, rising time, temperature, liquid-to-solid ratio, and holding time were selected as per the review and preliminary trails. The effects of a suitable solvent (N<sub>A</sub>DES), its concentration in water (10, 30, 50, 75, and 85%), rising time (5, 15, 25, 35, and 45 min), temperature (15, 35,

**Table 1. Compositions of Different N<sub>A</sub>DES**

Types of N <sub>A</sub> DES <sub>s</sub>	Hydrogen Bond Acceptor (HBA)	Hydrogen Bond Donor (HBD)	Molar Ratio	Viscosity <sup>a</sup> (mPa.s)
N <sub>A</sub> DES -I	ChCl	Urea	1:2	138
N <sub>A</sub> DES-II	ChCl	Ethylene glycol	1:2	278
N <sub>A</sub> DES -II	ChCl	Lactic acid	1:2	132
N <sub>A</sub> DES-IV	ChCl	Maltose	1:2	221

<sup>a</sup>Measured at 24 ± 2 °C.

55, 75, and 95 °C), liquid-to-solid ratio (10, 25, 40, 55, and 70 mL/g), and holding time (5, 15, 25, 35, and 45 min) on the extraction yield, antioxidant activity, TPC, and TFC from orange peel were examined using the OFAT method. The FCCD model was applied through response surface methodology to choose and set the optimized values of each parameter, including NADES concentration in water, rising time, temperature, liquid-to-solid ratio, and holding time, which were determined by the OFAT method.

**2.4. Experimental Design.** Using FCCD with six center points, the impact of the four independent variables: rising time ( $X_1$ ), temperature ( $X_2$ ), liquid-to-solid ratio ( $X_3$ ), and holding time ( $X_4$ ), on the dependent variables, extraction yield, DPPH, ABTS, TPC, and TFC, was determined. Thirty tests in total were carried out according to the experimental plan provided by the Design Expert software (Version 13.0.1). A second-order model eq (eq 1) was used to assess the model's adequacy with  $R^2$ , adjusted  $R^2$ , predicted  $R^2$  and Fisher's test.

$$Y = \beta_0 + \sum_{i=1}^n \beta_i X_i + \sum_{i=1}^n \beta_{ii} X_i^2 + \sum_{i=1}^{n-1} \sum_{j=i+1}^n \beta_{ij} X_i X_j \quad (1)$$

where  $X$ ,  $Y$ ,  $\beta_0$ ,  $\beta_i$ ,  $\beta_{ii}$ , and  $\beta_{ij}$  represent independent parameters, responses, and regression coefficients, respectively.

**2.5. Experimental Approach.** **2.5.1. MA-N<sub>A</sub>DESE.** A microwave extractor (Ethos, Milestone, Italy) equipped with an easy-to-control software setup for 3-level control of the irradiation time and temperature was used for all the experiments under different processing conditions (Table 2). Briefly, in 1 g of peel powder was added 20 mL of N<sub>A</sub>DESE-II and mixed well. Microwave treatment was applied according to the criteria given in Table 1. Following the MAE procedure, Whatman No. 1 filter paper was used to filter the sample. Next, using a rotary evaporator (Buchi Rotavapor R-200, Switzerland), the filtrate was condensed at 50 °C and filtered using a vacuum pump. Until further analysis, the crude extract was kept in a refrigerator at 4 °C.

**2.5.2. Conventional (Heating-Stirring) Extractions.** For heating-stirring extraction (HSE), 20 mL of N<sub>A</sub>DESE-II was mixed with 1 g of peel powder, and the mixture was stirred (500 rpm) at 50 °C for 30 min. After the HSE process, the treated sample was filtered through filter paper (Whatman No. 1), and the filtrate was condensed at 50 °C using a rotary evaporator (Buchi Rotavapor R-200, Switzerland) and filtered using a vacuum pump. The crude extract was stored in a refrigerator at 4 °C until further analysis.

**2.6. Analytical Approaches for Responses.** **2.6.1. Total Extract Yield.** Following extraction, the total extract yield was calculated using the eq (eq 2) given below.

$$\text{extract yield (\%)} = \frac{W_E}{W_S} \times 100 \quad (2)$$

Table 2. Experimental Conditions and Results as per FCCD

Run	Factor 1	Factor 2	Factor 3	Factor 4	Response 1	Response 2	Response 3	Response 4	Response 5
	X <sub>1</sub> :Time (min)	X <sub>2</sub> :Temp (°C)	X <sub>3</sub> :L/S (mL/g)	X <sub>4</sub> :Holding Time (min)	Yield (%)	DPPH (%)	ABTS (%)	TPC (mg GAE/g)	TFC (mg QAE/g DW)
1	40	90	20	10	24.01	30.54	43.10	41.73	33.56
2	25	30	40	20	31.54	73.30	72.16	49.01	53.87
3	25	60	40	20	36.50	74.02	86.92	69.66	71.16
4	25	60	40	20	34.04	74.30	78.26	71.08	71.91
5	40	60	40	20	33.54	76.11	87.54	64.63	57.13
6	40	30	20	30	35.01	70.24	68.80	51.01	41.12
7	10	30	60	10	32.08	36.13	45.23	39.54	48.16
8	25	60	40	20	37.01	76.72	89.86	73.02	72.86
9	10	30	20	10	33.79	61.39	64.36	55.57	44.02
10	10	30	20	30	35.46	65.55	63.54	55.21	42.02
11	40	90	60	10	25.97	31.93	39.63	42.26	34.87
12	25	60	40	20	35.02	71.12	79.37	70.45	73.36
13	25	60	40	10	30.17	41.54	41.11	66.60	73.28
14	25	90	40	20	26.04	52.82	64.02	47.15	37.71
15	25	60	40	30	34.41	60.87	61.01	72.92	74.05
16	25	60	20	20	36.23	68.54	79.27	76.20	73.03
17	10	90	60	30	28.61	56.02	73.17	56.43	35.64
18	10	60	40	20	34.02	75.30	85.26	64.25	53.08
19	40	30	60	30	25.48	51.83	59.06	46.84	52.68
20	10	90	60	10	24.12	33.63	39.01	36.26	33.03
21	10	30	60	30	32.91	54.57	62.62	50.02	48.15
22	10	90	20	10	18.54	23.27	38.82	36.02	31.03
23	10	90	20	30	26.41	48.24	59.02	48.48	33.12
24	40	90	60	30	27.96	59.57	68.75	64.72	34.23
25	40	30	60	10	27.74	39.21	53.72	40.32	56.62
26	40	90	20	30	31.02	45.57	61.01	52.71	30.17
27	25	60	60	20	33.82	62.36	74.02	77.57	76.67
28	40	30	20	10	33.87	60.54	76.23	53.37	51.02
29	25	60	40	20	34.04	75.52	89.02	73.86	73.88
30	25	60	40	20	35.17	72.08	79.27	70.54	71.62

Where,  $W_E$  and  $W_S$  represent the weight of dry extract and weight of sample, respectively.

### 2.6.2. Determination of Antioxidant Capacity.

**2.6.2.1. DPPH Assay.** The methodology reported by Kumar et al.<sup>15</sup> was used for the 2,2-diphenyl-1-picrylhydrazyl (DPPH) assay. In 1 mL of different concentrations of  $N_ADES_s$  extract (1–20 mg/mL), 4.0 mL of DPPH (0.004%) was mixed. Absorbance was recorded after 30 min of incubation using a UV spectrophotometer (Hitachi U-1800, Japan) at 517 nm. The following eq (eq 3) was used to compute the radical scavenging activity:

$$\text{DPPH Scavenging activity (\%)} = \frac{A_C - A_S}{A_C} \times 100 \quad (3)$$

where  $A_C$  and  $A_S$  are the absorbance of control and sample, respectively.

**2.6.2.2. ABTS Radical Scavenging Activity.** Uysal et al.<sup>16</sup> methodology was adopted for the determination of ABTS radical scavenging activity. One mL of  $N_ADES_s$  extract was mixed with 2 mL of ABTS, and this mixture was then left for 30 min at room temperature. After incubation, the absorbance was measured at 734 nm by using a UV spectrophotometer (Hitachi U-1800, Japan). The following eq (eq 4) was used to determine the ABTS scavenging activity:

$$\text{ABTS Scavenging activity (\%)} = \frac{A_C - A_S}{A_C} \times 100 \quad (4)$$

where  $A_C$  and  $A_S$  are the absorbance of control and sample, respectively.

**2.6.2.3. TPC.** Kumar et al.<sup>17</sup> method for TPC determination was adopted with slight modifications. Briefly, 1.5 mL of  $Na_2CO_3$  (20%) and 0.5 mL of Folin–Ciocalteu (10%) were mixed with 0.5 mL of  $N_ADES_s$  extract and vortexed for 2–3 min. Using distilled water, a total 10 mL volume was prepared, and perfect mixing was achieved by vortexing once again. The absorbance was taken at 725 nm using a UV spectrophotometer (Hitachi U-1800, Japan) after 40–45 min of incubation in the dark. The data were calculated as mg GAE/g using a standard calibration curve for gallic acid ( $Y = 0.0005x$ ;  $R^2 = 0.99$ ).

**2.6.2.4. TFC.** The methodology described by Van Hung et al.,<sup>18</sup> was used with slight modifications for the determination of TFC.<sup>17,19</sup> 0.5 mL of  $N_ADES_s$  extract and 0.3 mL of  $NaNO_3$  (5%) were mixed for 5 min, then 0.3 mL of  $AlCl_3$  (1%) was added to the mixture, and it was mixed again for 6 min. After adding 2 mL of 1 M NaOH, the final volume was made up to 10 mL using distilled water. The absorbance was recorded immediately afterward at 510 nm using a UV spectrophotometer (Hitachi U-1800, Japan). The results were calculated as mg QAE/g DW using a Quercetin standard calibration curve ( $y = 0.112x + 0.178$ ,  $R^2 = 0.99$ ).

**2.7. Optimization of Process Parameters.** The numerical and graphical (3D surface plot) optimization of the levels of rising time, temperature, liquid-to-solid ratio, and holding

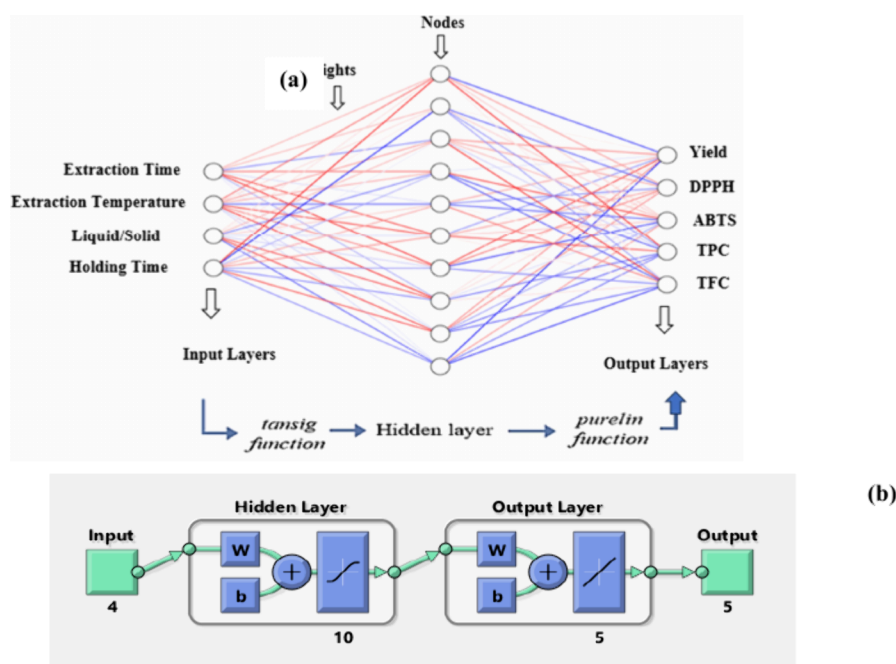


Figure 1. (a) Neural network architecture (NNA) (b) Overall experimental data set based generated network.

time was carried out using the FCCD model of RSM. Design Expert Software (Version 13.0.1) was used to carry out the optimization. The analysis of variance (ANOVA),  $R^2$ , adjusted  $R^2$ , predicted  $R^2$ , LOF, and CV were used for obtaining the optimal conditions for process parameters. During the process of optimization among all possible solutions, only one that met the criteria the most and had high desirability was selected.

#### 2.7.1. Artificial Neural Network (ANN) Approach.

**2.7.1.1. ANN Modeling Technique.** ANN methods were used to predict the extraction parameters of the experimental combination generated by RSM. While extraction time, temperature, liquid-to-solid ratio, and holding time were the input layers, the output layers included yield, DPPH, ABTS, TPC, and TFC content. A two-layer feed-forward network with hidden neurons having sigmoid function and output neurons having linear function was used in the current study. The experimental design suggested the use of 30 samples, which were split into training (70%), testing (15%), and validation (15%) groups. The multilayered perceptron (MLP) and back-propagation (BP) techniques were used to calculate the ANN model. The weight and bias variables were updated by using the network training function of the Levenberg–Marquardt method. Figure 1 depicts the network architectures of several neurons' hidden layers. In addition, the correlation established through regression analysis for each output parameters were validated using an ANN computation with three-layered feedforward backpropagation. The Purelin and logistic sigmoid transfer functions, which are believed to produce the best outcomes for activation functions for ANNs, were applied to the hidden and output layers. The number of neurons in the hidden layer was estimated by using trial-and-error techniques based on the regression coefficient. The weights for each trail were determined while taking into account the learning rate, which is a variable that changes during the training phase. By decreasing the variation between the neural network and the expected outputs, an optimal design was found. A description of the tansig sigmoidal and purelin functions that were utilized in the neural network

training for the current study has been provided in Equations 5 and 6.

$$\text{tansig}(x) = f(x) = 2.0 \left( \frac{1}{1 + e^{-\lambda x}} - 0.5 \right) \quad (5)$$

$$\text{Purelin}(x) = x \quad (6)$$

where  $\lambda$  is the slope parameter, which controls the slopes for the activation function. Using the constructed model's weights and bias values. The elaboration of eq (eq 7) given by Patra et al.<sup>20</sup> was utilized to predict each individual's response ( $Y_i$ ).

$$Y_i = \text{purelin}\{W_{HO} \times \tan \text{sig}(U_{IH} \times X_i \times TH) + TO\} \quad (7)$$

$X_i$  and  $Y_i$  represent the input and anticipated values of the output parameters, respectively. The  $U_{IH}$  and  $W_{HO}$  represent the weights between the hidden and input layers and the hidden and output layers, respectively. The hidden layer and output neurons' bias values are TH and TO, respectively.

**2.7.1.2. Conduction and Investigation of the Developed Models.** The developed models' performance was assessed and compared through RSM and ANN using a variety of statistical measures, including the root-mean-square error (RMSE), coefficient of determination ( $R^2$ ), mean absolute error (MAE), chi-square ( $\chi^2$ ), and average absolute deviation (ADD). Equations (eq 8) to (eq 12) were used to calculate the statistical parameters that were employed for the model analysis.<sup>21,22</sup>

$$R^2 = 1 - \frac{\sum_{i=1}^n (Y_{pi} - Y_{ai})^2}{\sum_{i=1}^n (Y_{pi} - Y_m)^2} \quad (8)$$

$$\text{RSME} = \sqrt{\frac{1}{n} \sum_{i=1}^n (Y_{pi} - Y_{ai})^2} \quad (9)$$

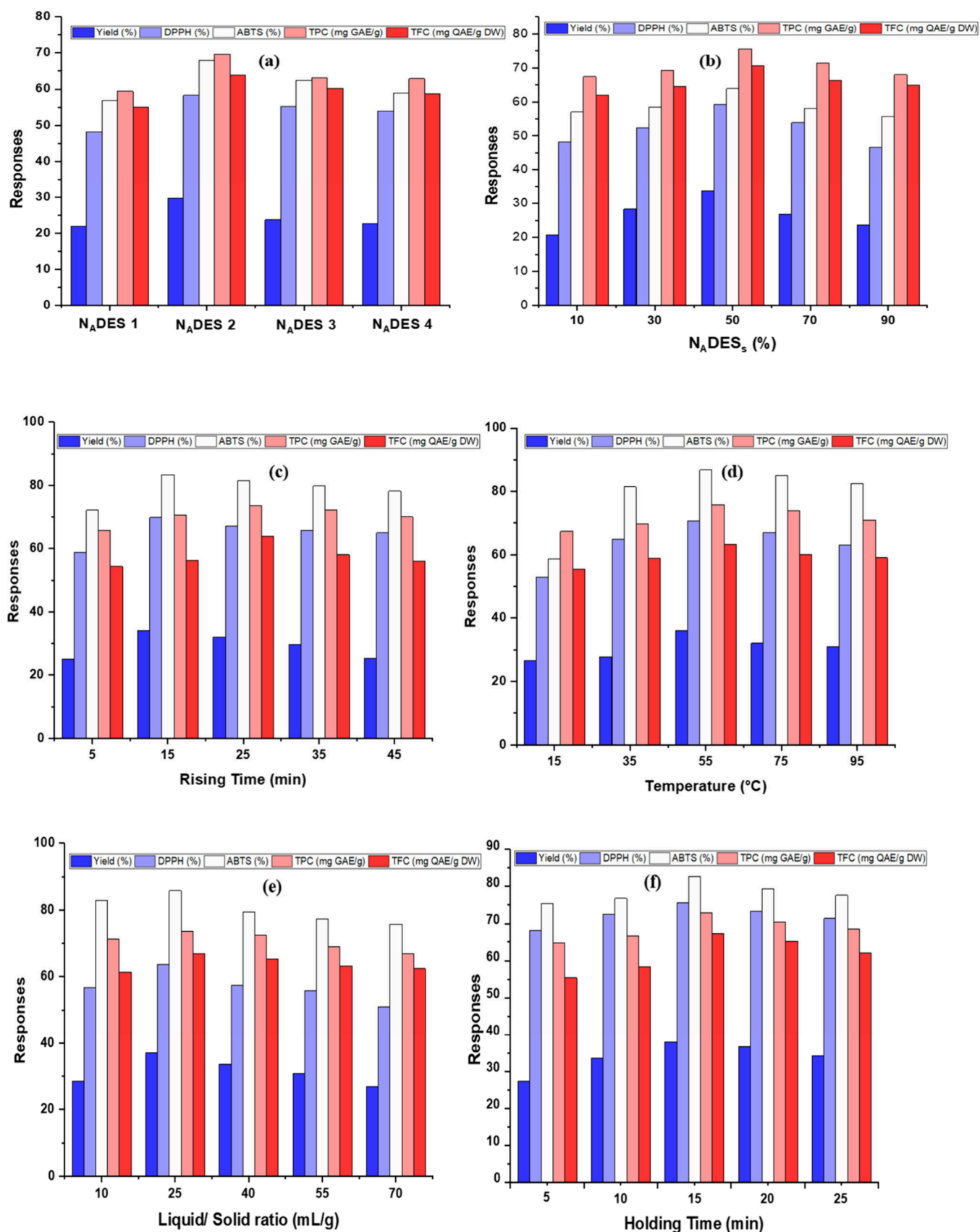


Figure 2. One-factor-at-a-time experimental results showing (a) NADES variation, (b) NADES% variation, (c) rising time variation, (d) temperature variation, (e) liquid-to-solid ratio variation, and (f) holding-time variation for the microwave-assisted extraction of orange peel.

Table 3. ANOVA for Response Surface Polynomial Model of All Independent Variable<sup>a</sup>

Source	Yield (%)		DPPH (%)		ABTS (%)		TPC(mg/g)		TFC (mg QAE/g DW)	
	F-value	p-value	F-value	p-value	F-value	p-value	F-value	p-value	F-value	p-value
Model	34.54	<0.0001	51.1	<0.0001	20.36	<0.0001	151.73	<0.0001	217.1	<0.0001
X <sub>1</sub> -Rising Time	0.0802	0.7808	0.714	0.4114	1.62	0.2222	6.03	0.0268	11.48	0.0041
X <sub>2</sub> -Temp	136.87	<0.0001	93.9	<0.0001	14.16	0.0019	5.52	0.0329	386.93	<0.0001
X <sub>3</sub> -L/S	10.99	0.0047	12.9	0.0027	3.42	0.0843	6.42	0.0229	35.96	<0.0001
X <sub>4</sub> -Holding Time	32.69	<0.0001	129.93	<0.0001	41.57	<0.0001	181.01	<0.0001	4.47	0.0517
X <sub>1</sub> X <sub>2</sub>	27.72	<0.0001	0.0316	0.8613	0.9746	0.3392	29.6	<0.0001	8.78	0.0097
X <sub>1</sub> X <sub>3</sub>	20.75	0.0004	0.2406	0.6308	1.26	0.2796	1.89	0.1891	1.46	0.2463
X <sub>1</sub> X <sub>4</sub>	2.47	0.1366	0.1509	0.7031	1.72	0.2099	0.7178	0.4102	10.21	0.006
X <sub>2</sub> X <sub>3</sub>	35.76	<0.0001	73.66	<0.0001	12.76	0.0028	94.95	<0.0001	7.44	0.0156
X <sub>2</sub> X <sub>4</sub>	20.20	0.0004	12.5	0.003	19.17	0.0005	72.73	<0.0001	6.58	0.0215
X <sub>3</sub> X <sub>4</sub>	8.07	0.0124	4.56	0.0497	8.01	0.0127	41.01	<0.0001	3.03	0.1021
X <sub>1</sub> <sup>2</sup>	0.0347	0.8547	8.59	0.0103	10.59	0.0053	41.44	<0.0001	223.67	<0.0001
X <sub>2</sub> <sup>2</sup>	54.90	<0.0001	11.9	0.0036	7.22	0.0169	565.47	<0.0001	589.37	<0.0001
X <sub>3</sub> <sup>2</sup>	2.62	0.1265	5.04	0.0403	0.0081	0.9297	45.66	<0.0001	22.98	0.0002
X <sub>4</sub> <sup>2</sup>	5.53	0.0328	88.91	<0.0001	64.41	<0.0001	0.6226	0.4424	13.02	0.0026
LOF	0.716	0.6953	3.01	0.118	0.7785	0.6568	0.7876	0.6513	2.94	0.1231
CV%	3.57		5.56		7.51		2.65		3.05	
PRESS	57.3		712.37		912.01		124.9		147.86	
R <sup>2</sup>	0.97		0.9795		0.95		0.993		0.9951	
Adjusted R <sup>2</sup>	0.94		0.9603		0.90		0.986		0.9905	
Predicted R <sup>2</sup>	0.91		0.9042		0.87		0.975		0.9813	
Adeq Precision	23.2		23.587		15.45		39.56		42.7768	
AAD	0.585		1.9		2.521		0.833		0.83	
MSE	0.618		5.1		12.84		1.151		1.29	
RSME	0.786		2.3		3.582		1.073		1.14	
MPE	0.018		0.1		0.171		0.017		0.02	

<sup>a</sup>LOF: Lack of Fit; CV: Coefficients of variation; AAD: average absolute deviation; MSE: mean square error; RSME: root-mean-square error; MPE: mean percentage error.

$$\text{MAE} = \frac{1}{n} \sum_{i=1}^n |Y_{pi} - Y_{ai}| \quad (10)$$

$$\chi^2 = \sum_{i=1}^n \frac{(Y_{pi} - Y_{ai})^2}{Y_{pi}} \quad (11)$$

$$\text{AAD}(\%) = \left[ \frac{\sum_{i=1}^n (|Y_{pi} - Y_{ai}|/Y_{pi})}{n} \right] \times 100 \quad (12)$$

where  $n$  = experimental number,  $Y_{pi}$  = predicted and  $Y_{ai}$  = experimental value,  $Y_m$  = average experimental value.

### 3. RESULTS AND DISCUSSION

**3.1. Screening of Process Parameters Using OFAT Approach.** Six process variables, including the appropriate solvent (N<sub>A</sub>DES), the percentage of N<sub>A</sub>DES in the water, the rising time, the extraction temperature, the liquid-to-solid ratio, and the holding time, were examined for their effects on the extraction yield, antioxidant activity, TPC, and TFC of the orange peel. The results of the OFAT approach are depicted in Figure 2.

The antioxidant content of the orange peels was extracted using four distinct types of N<sub>A</sub>DES<sub>s</sub> (Table 1). According to the findings, N<sub>A</sub>DES-II (choline chloride: ethylene glycol) outperformed all other N<sub>A</sub>DES<sub>s</sub> in terms of maximal extraction yield, greater DPPH and ABTS scavenging activity, TPC, and TFC (Figure 2(a)). The extraction efficiency greatly depends on the concentration of N<sub>A</sub>DES in the water.<sup>23</sup> From Figure

2(b), it was observed that the dissolution and penetration of antioxidants were maximum at a 50% concentration of N<sub>A</sub>DES-2 in water; beyond this, the high viscosity of the target matrix limited the dissolution and penetration of antioxidants. Based on the results in Figure 2(a) and (b), it was concluded that the best N<sub>A</sub>DES solvent and % N<sub>A</sub>DES in water were N<sub>A</sub>DES-II (ChCl: Ethylene Glycol), and 50% water, respectively. Thus, subsequent experiments were performed using N<sub>A</sub>DES-2 with 50% water.

The other four process parameters, including rising time (10 to 40 min), temperature (30 to 90 °C), liquid-to-solid ratio (20 to 60 mL/g), and holding time (10 to 30 min), were also investigated and screened using the OFAT approach for the optimization of extraction yield, antioxidant activity, TPC, and TFC from orange peel.

The impact of rising time, temperature, liquid-to-solid ratio, and holding time on extraction yield, antioxidant activity, TPC, and TFC are depicted in Figure 2(c), (d), (e), and (f) respectively. The extraction yield, antioxidant activity, TPC, and TFC all increased after 15 min; however, any additional time spent increased the responses. According to Dahmoune et al.,<sup>24</sup> this might be the result of the peel matrix being exposed to microwave radiation, which might cause the thermal degradation of the antioxidant molecules that are responsible for the antioxidant activity of the extract. As a result, the optimization experiment chose a rising time range of 10 to 40 min.

Temperature plays a significant role in the extraction of antioxidants. From Figure 2(d), it was noticed that the extraction yields, along with higher antioxidant activities, TPC

and TFC increased with an increasing temperature from 10 to 55 °C. The mass transfer acceleration brought on by higher temperatures can be used to explain this rise in extraction yield.<sup>20</sup> Further increases in the temperature led to a decrease in values (Figure 2(d)). An excessively high temperature can reduce activity, damage the target compounds, and make impurities more soluble, lowering the extraction yield.<sup>25</sup> The temperature range of 30 to 90 °C was finally selected for the RSM design.

The extraction yield, antioxidant activity, TPC, and TFC all showed significant improvements when the liquid-to-solid ratio was raised from 10 to 20 mL/g (Figure 2(c)). However, any additional increase over 25 mL/g had a negative effect on these properties. This might be because when microwaves are used the increased volume of solvent is improperly stirred. Furthermore, absorbing more microwave energy from a higher amount of solvent may result in inadequate energy to effectively breakdown the phenolic compounds of the cell walls.<sup>26</sup> A 20–60 mL/g liquid-to-solid ratio was selected for the RSM design. The extraction yield, antioxidant activity, TPC, and TFC were markedly enhanced when the microwave holding period was prolonged from 5 to 25 min, as shown in Figure 2(f). The extraction yield, antioxidant activities, TPC, and TFC were significantly decreased after 25 min. The mass transfer of intracellular bioactive chemicals may have been sped up by extending the microwave holding period past 25 min. However, an excessive amount of microwave holding time can result in the antioxidant content degrading.<sup>24</sup> As a result, the RSM design was chosen with a microwave holding time range of 10 to 30 min.

**3.2. Model Fitting and Adequacy of Experimental Data.** The obtained results of the study are depicted in Table 2, whereas Table 3 depicts the results of ANOVA for experimental values, viz., mean square error (MSE), average absolute deviation (AAD), mean percentage error (MPE), root-mean-square error (RSME),  $R^2$ , adj $R^2$ , predicted  $R^2$ , adequate precision, coefficient of variation (C.V.%), and lack of fit. An  $R^2$  value of greater than 85% explained a strong relationship between the experimental and predicted values.<sup>27</sup> The  $R^2$  values in this study were noted as 97%, 97.95%, 95%, 93.90%, and 99.51% for the extraction yield, DPPH, ABTS, TPC, and TFC, respectively. The values of  $R^2$  and adj- $R^2$  closer to 100% indicated that the empirical model fit the experimental data with a nonsignificant ( $p < 0.05$ ) lack of fit.<sup>28</sup> In the current study, the adequate precision values of 23.20, 23.58, 15.45, 39.56, and 42.77 for extraction yield, DPPH, ABTS, TPC, and TFC, respectively, which were higher than 4 indicate that the current model may be utilized. The authenticity of the experiment depends on its CV value; i.e., the lower the value, the higher the authenticity. Results of the study indicate that the lower CV (%) values, i.e., 3.57, 5.56, 7.51, 2.65, and 3.05 for extraction yield, DPPH, ABTS, TPC, and TFC, respectively, indicate greater experimental authenticity.<sup>29,30</sup> An analysis of the regression coefficient was performed to determine the statistical significance of the model terms (Table S1).

**3.3. Effect of MAE on Extraction Yield (%).** The microwave-assisted extraction yield of orange peel was found to be in the range of 18.54% to 37.01% irrespective of the experimental combinations (Table 2). The minimum yield of 18.54% was obtained at a 10 min rising time ( $X_1$ ), 90 °C temperature ( $X_2$ ), 20 mL/g liquid-to-solid ratio ( $X_3$ ), and holding time ( $X_4$ ) of 10 min, whereas the maximum yield

(37.01%) was noticed at 25 min rising time ( $X_1$ ), 60 °C temperature ( $X_2$ ), 40 mL/g liquid-to-solid ratio ( $X_3$ ), and holding time ( $X_4$ ) of 20 min (Table 2).

Extraction yield is greatly improved by the effects of linear terms like  $X_4$  ( $p < 0.001$ ) and interaction terms such as  $X_1X_2$ ,  $X_2X_3$ , and  $X_2X_4$  ( $p < 0.001$ ) (Table 3). The model's higher  $F$  value (34.54) suggests the significance of the design model ( $p < 0.01$ ) (Table 3).

The impacts of MAE process parameters on extraction yield are depicted by the 3D response graphs in Figure S1(a), (b), and (c). These figures show a decrease in extraction yield with increasing temperature as well as with an increasing liquid-to-solid ratio. This may be explained by an increase in the sample's electric field and the rate of heating in the solvent, both of which lead the bioactive compounds to degrade thermally.<sup>31</sup> Similar results were noted when baicalin was extracted from *Scutellaria baicalensis* Georgi.<sup>25</sup> The length of the extraction process is known to generally increase the extraction yield, although the growth decreases after a certain time.<sup>30,31</sup> The extraction yield increased somewhat with extended holding times, as can be observed in Figure 2(c). This phenomenon may be attributed to the sequential steps: the solid sample absorbing the solvent, the dissolution of soluble components by the solvent, and the subsequent release of the solvent along with the dissolved components.<sup>32–34</sup> Similar findings were reported by Doulabi et al.,<sup>35</sup> who observed that lengthening the extraction process improved the quantity of bioactive chemicals in eggplant.

**3.4. Effect of Microwave Treatment on DPPH (%).** The simplest technique to assess the antioxidant capacity of plant materials is to measure their DPPH radical scavenging activity.<sup>36</sup> The DPPH value varied from a minimum of 23.27% to a maximum of 76.72% (Table 2). With an  $F$ -value of 51.1, the overall fitted model for DPPH from ANOVA (Table 3) was found to be significant ( $p < 0.001$ ). The negative effect of temperature ( $X_2$ ) ( $p < 0.001$ ), and liquid-to-solid ratio ( $X_3$ ) ( $p < 0.001$ ) on the antiradical activity of orange peel, and a positive effect of microwave rising ( $X_1$ ) and holding time ( $X_4$ ) ( $p < 0.001$ ) on DPPH radical scavenging activity has been depicted in Table S1. Statistically, the interaction terms  $X_1X_2$ ,  $X_2X_3$  ( $p < 0.001$ ),  $X_2X_4$  ( $p < 0.001$ ) and  $X_3X_4$  ( $p < 0.05$ ) and the quadratic terms  $X_1^2$  ( $p < 0.01$ ) showed a significantly positive effect on antiradical activity. The combined effects of  $X_2X_3$  significantly ( $p < 0.001$ ) impacted the antioxidant activity of orange peel.

It can be clearly observed from Figure S2 (a), (b), and (c) that the DPPH radical scavenging activity decreased with increasing the liquid-to-solid ratio ( $X_3$ ) and temperature ( $X_2$ ) while increasing with increasing holding time ( $X_4$ ). According to Hayat et al.,<sup>37</sup> with an increase in microwave extraction time for 5- to 10 min, the DPPH radical scavenging activity of citrus mandarin peel powder increased from 17.96 to 26.96%. Kumar et al.<sup>38</sup> also reported a significant increase in the antioxidant activity of microwave-treated coriander paste with an increase in heating time.

**3.5. Effect of Microwave Treatment on ABTS (%).** Based on the ABTS+ assay, the antioxidant value ranged from 38.82 to 89.86% (Table 2). With an  $F$ -value of 20.36, the overall fitted model for ABTS using ANOVA (Table 3) was found to be significant ( $p < 0.001$ ). Linear terms such as rising time ( $X_1$ ) and holding time ( $X_4$ ) had a significant effect on ABTS content (Table S1). The interaction effect was significantly negative for  $X_1X_2$ ,  $X_1X_3$ , and  $X_1X_4$  and significantly

positive for  $X_2X_3$  ( $p < 0.01$ ),  $X_2X_4$  ( $p < 0.001$ ),  $X_3X_4$  ( $p < 0.01$ ). Furthermore, the quadratic terms such as  $X_1^2$  ( $p < 0.01$ ) showed a significant positive effect, and  $X_2^2$  ( $p < 0.01$ ),  $X_4^2$  ( $p < 0.001$ ) showed a significant negative effect.

The response surface curve in Figure S3 (a), (b), and (c) depicts the effect of process parameters on ABTS<sup>+</sup> activity. It can be clearly observed from Figure S3 (a), (b), and (c) that the antioxidant activity in terms of the ABTS<sup>+</sup> assay increased initially with increasing the microwave temperature ( $X_2$ ) and holding time ( $X_4$ ) and further decreased after certain levels of temperature and holding time. This may be due to the transmigration of dissolved molecules caused by the rapid heating of the entire plant matrix by microwaves. Additionally, microwave irradiation improves the solubility of bioactive compounds and solvent absorption into the matrix.<sup>39</sup> Bhuyan et al.<sup>40</sup> reported that the ABTS scavenging activity of eucalyptus *robusta* leaf MAE increases with an increase in holding time.

**3.6. Effect of Microwave Treatment on TPC.** The TPC of orange peel ranged for the selected experimental combinations from 36.02 to 77.57 mg of GAE/g (Table 2). The overall fitted model for TPC using ANOVA (Table 3) had a significant ( $p < 0.05$ )  $F$ -value of 151.73. A significant positive effect of rising time ( $X_1$ ) ( $p < 0.05$ ) and holding time ( $X_4$ ) ( $p < 0.001$ ) was observed on the TPC content. Among the quadratic terms,  $X_1^2$  ( $p < 0.001$ ) and  $X_2^2$  ( $p < 0.001$ ) had significant negative effects, whereas  $X_3^2$  ( $p < 0.001$ ) had a significant positive effect on the TPC value (Table S1). The effect of interaction terms on TPC content was found to be statistically significant at a 1% level of significance with the exception of  $X_1X_3$  and  $X_1X_4$  (Table S1).

The 3D response graphs in Figure S4 (a), (b), and (c) demonstrate the impact of MAE process parameters on TPC. In the current study, with the increase in temperature from 30 to 90 °C, the TPC first increased up to 60 °C and then subsequently decreased, as shown in Figure S4 (a). It might be brought on by the degradation of polyphenolic components at temperatures above 60 °C.<sup>41</sup> As the extraction temperature increases to 60 °C, phenolic compounds' solubility and diffusion in the extraction solvent may increase. The TPC decreased slightly with an increase in liquid-to-solid ratio (Figure S4 (b)). Enough solvent can cause materials to expand, making it easier to rupture the cell walls and finally extract the polyphenols. However, using too much solvent can have the opposite effect. Because solids absorb less microwave radiation, the amount of phenolic chemicals that can be extracted is reduced.<sup>35</sup> Figure S4 (c), which indicates the effect of holding time, shows that the TPC increased as holding time increased. This might happen as a result of prolonged extraction durations, potentially destroying the majority of the cell walls and releasing phenolic compounds into the solvent. The findings of the present study are consistent with those of previous research conducted by Kumar et al.<sup>42</sup>

**3.7. Effect of Microwave Treatment TFC.** The TFC of the bioactive compound ranged from 31.04 to 76.68 mg of QAE/g of DW for the selected experimental combinations (Table 2). The overall fitted model for TFC using ANOVA (Table 3) had a significant ( $p < 0.001$ )  $F$ -value of 217.1. The TFC of orange peel extract was significantly affected by the linear terms, viz., rising time ( $X_1$ ) ( $p < 0.001$ ), temperature ( $X_2$ ) ( $p < 0.001$ ), liquid-to-solid ratio ( $X_3$ ) ( $p < 0.001$ ), and holding time ( $X_4$ ) ( $p < 0.05$ ). The coefficients of  $X_1$  and  $X_3$  are positive while  $X_2$  and  $X_4$  are negative, indicating an increase in

the flavonoid compound of orange peel with an increase in microwave rising time ( $X_1$ ) and liquid-to-solid ratio ( $X_3$ ) (Table S1). Among the quadratic terms,  $X_1^2$  ( $p < 0.001$ ) and  $X_2^2$  ( $p < 0.001$ ) had a significant negative effect, while a significant positive effect of  $X_3^2$  ( $p < 0.001$ ), and  $X_4^2$  ( $p < 0.01$ ) is observed on the TFC value. Except for  $X_1X_3$  and  $X_3X_4$ , the effect of interaction terms on the TFC content was statistically significant (Table S1).

The 3D response graphs shown in Figure S5 (a), (b), and (c) indicate the effects of process parameters of MAE on TFC. With the increasing liquid-to-solid ratio and holding time, the TFC was also slightly increased. According to Alara et al.,<sup>31</sup> the TFC increased as the liquid-to-solid ratio increased when a bioactive component was extracted from *Vernonia cinerea* leaves. The solute–solvent interaction was affected by the holding time, which increased the extraction yield.<sup>41</sup> The flavonoid content initially increased with an increase in microwave temperature and further decreased (Figure S5 b). Ghafoor et al.<sup>43</sup> and Xiao et al.<sup>44</sup> reported similar observations while extracting TFC from *Radix Astragalii*.

**3.8. Model Validation.** The target goals for the process parameters and MA-NADESE responses were chosen and fixed for numerical optimization. Table 4 shows the optimal process

**Table 4. Experimental Data on Verification of Optimal Results**

Dependent variables	Predicted value	Experimental value	Error%
Yield (%)	37.01	36.28	−1.97
DPPH (%)	76.47	74.63	−2.40
ABTS (%)	87.80	85.31	−2.83
TPC (mg GAE/g)	74.73	71.03	−4.95
TFC (mg QAE/g DW)	63.86	60.75	−4.87

parameter values and corresponding responses produced using Design-Expert software (ver. 13.0.1). The optimal MA-NADESE conditions were 13.26 min of rising time, 52.96 °C of temperature, liquid-to-solid ratio of 20 mL/g, and 21.63 min of holding time. The projected values of responses, i.e., extraction yield, antioxidant capabilities of DPPH and ABTS, TPC, and TFC under the optimal conditions, were 37.01%, 76.47%, 87.80%, 74.73 mg of GAE/g, and 63.86 mg of QAE/g, respectively. The experimental values obtained at optimal conditions were 36.28 ± 1.01%, 74.63 ± 1.03%, 85.31 ± 1.02%, 71.03 ± 1.06 mg GAE/g, and 60.75 ± 1.08 mg QAE/g (Table S1). In this study due to no significant discrepancies between the experimental and anticipated values ( $p > 0.05$ ), the values were found to be in reasonable agreement with the expected values when evaluated using a paired  $t$  test. It was consequently concluded that the models were appropriate for this investigation.

**3.9. ANN Modeling.** The “ANN tool” was used to conduct ANN modeling. Using the experimental design of the process variables, the data sets were trained to predict the responses. The model was designed and trained by using experimental data. The data set was trained using a feedforward back-propagation network structure with 3 layers: the input layer, the hidden layer, and the output layer. The activation function (Tansig sigmoid transfer function) was selected between the input and hidden layers. The purelin function was chosen for prediction in the hidden and the output layers. The network included 4 input neurons (Extraction Time, Temperature, Liquid-to-Solid Ratio, and Holding Time) and output neurons



**Table 5. Optimum ANN Structure Topologies and Their Statistical Predictors**

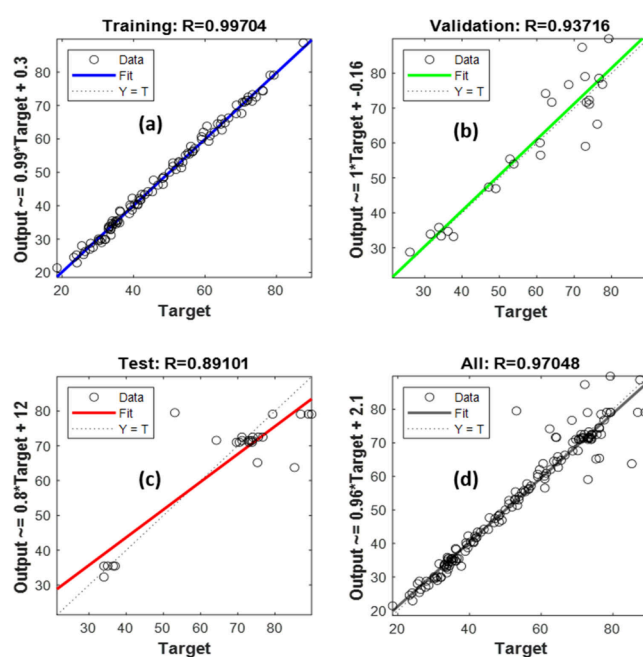
Response parameters	Network	Training algorithm	Threshold function	Network topology	(R)	MSE
Yield (%)	FFBP	LM	tansig-purelin	4-11-1	0.965	0.400
DPPH (%)					0.950	4.717
ABTS (%)					0.935	6.807
TPC (mg GAE/g)					0.950	1.071
TFC (mg QAE/g DW)					0.978	0.648

**Table 6. Comparison of Various Responses Using Statistical Parameters of RSM and ANN**

Prediction parameters	RSM					ANN				
	R <sup>2</sup>	RMSE	χ <sup>2</sup>	MAE	AAD%	R <sup>2</sup>	RMSE	χ <sup>2</sup>	MAE	AAD%
Yield	0.970	0.786	0.075	0.585	1.821	0.982	0.633	0.015	0.445	1.410
DPPH	0.979	2.301	0.423	1.948	3.714	0.983	1.234	0.198	1.523	2.576
ABTS	0.950	3.582	0.997	2.521	3.700	0.973	0.976	0.244	0.953	1.221
TPC	0.993	1.073	0.093	0.833	1.385	0.993	0.740	0.032	0.549	0.977
TFC	0.995	1.140	0.151	0.833	1.586	0.998	0.795	0.105	0.632	1.234

(Yield, DPPH, ABTS, TPC, and TFC) in the model. The input neurons and targeted neurons were used to create the neural network. The model neural architecture developed is shown in Figure 1 (a) and (b). Individual responses and overall data sets from the experiment are used to train network topologies for prediction. The network architecture model's initialization, random reverts of the weights, and the process parameters of the input neurons were integrated to train the neural network model. To determine the optimal number of neurons for individual as well as overall responses, statistical metrics such as the correlation coefficient ( $r$ ) and average square error (ASE) were used. As shown in Table 5, the neural network model's training used a range of neurons from 5 to 15. The optimized neuron was found to have a value of 11 for yield, DPPH, ABTS, TPC, and TFC, with respective correlation coefficient values of 0.965, 0.950, 0.935, 0.950, and 0.978. The root-mean square error (RMSE) and coefficient of determination ( $R^2$ ) for each individual response and the entire data set were determined to be between 0.633 and 1.234 and 0.973 and 0.998, respectively. Table 6 depicts a significant relationship between the experimental and predicted values. Furthermore, using a network topology of 4–11–1 and correlation coefficient values of 0.9704 for overall data sets, the optimal hidden layer neuron was 10. As shown in Figure 3, the overall performance of the data sets was evaluated using regression plots of the training, testing, and validation sample sets with correlation coefficient values.

**3.10. Comparative Analysis.** Statistical parameters are essential for assessing the performance of the developed model and its prediction. Based on its highest value being near 1, the coefficient of determination ( $R^2$ ) is primarily used to determine the fitness of the model. The coefficient of determination ( $R^2$ ) value was determined to be insufficient to examine the performance and correctness of the model due to the complicated phenomena of the numerous factors.<sup>45</sup> Figure 4 displays the regression of experimental and predicted values using the RSM and ANN approaches for the various responses. Other statistical factors may also be considered in order to forecast the exact performance of the model. Table 6 lists the additional statistical variables used in this study for predicting the model features based on their lowest values. These variables include RMSE,  $\chi^2$  value, MAE, and AAD. The  $R^2$  values between experimental and predicted values was observed to be 0.970, 0.979, 0.950, 0.993, and 0.995 for the

**Figure 3.** Correlation coefficients (a) training (b) validation (c) testing and (d) overall testing for the overall developed ANN model

RSM model and 0.982, 0.983, 0.973, 0.993, and 0.998 for the ANN model of yield, DPPH, ABTS, TPC, and TFC, respectively. Similarly, RMSE values were found to be 0.786, 2.301, 3.582, 1.073, and 1.140 for the RSM model and 0.633, 1.234, 0.976, 0.740, and 0.795 for the ANN model of yield, DPPH, ABTS, TPC, and TFC, respectively. Similar results are reported for additional statistical parameters such as  $\chi^2$ , MAE, and AAD% an appropriate range for accurately predicting the developed model. When the ANN predictive model is compared to the RSM model, these results demonstrate a higher  $R^2$  value and a lower RMSE value. In the same way, additional statistical metrics like  $\chi^2$ , MAE, and AAD% were found to be lower for the ANN model than for the RSM model, suggesting a superior prediction. Furthermore, the RSM and ANN models' statistical characteristics showed little change, suggesting that both models are capable of accurate response prediction. Elnjikkal and Dwivedi<sup>46</sup> found that for microwave vacuum drying of pomegranate peel, these

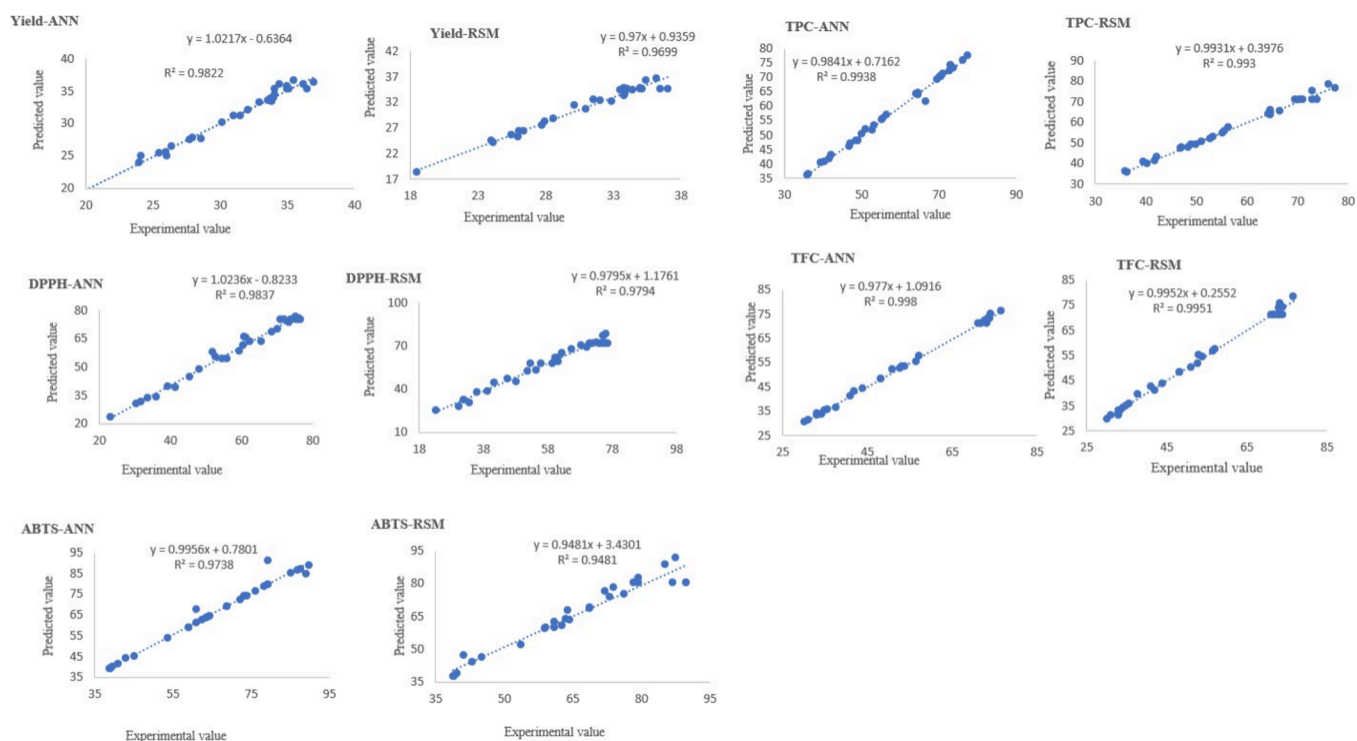


**Figure 4.** Comparative analysis of the ANN and RSM models.

outcomes are equivalent to an excellent ANN method prediction.

**3.11. Comparison of MA-N<sub>A</sub>DESE and HSE.** The comparison of MA-N<sub>A</sub>DESE and HSE was carried out at optimal conditions, i.e., 13 min of rising time, 53 °C of temperature, liquid-to-solid ratio of 20 mL/g, and a 21 min holding time. The experimental values of responses, i.e., extraction yield, antioxidant capabilities of DPPH and ABTS, TPC, and TFC obtained through MA-N<sub>A</sub>DESE and HSE processes at optimal conditions, were  $36.28 \pm 1.01\%$ ,  $74.63 \pm 1.03\%$ ,  $85.31 \pm 1.02\%$ ,  $71.03 \pm 1.06$  mg GAE/g, and  $60.75 \pm 1.08$  mg QE/g, and  $24.06 \pm 1.1\%$ ,  $53.01 \pm 2.02\%$ ,  $66.04 \pm 1.03\%$ ,  $56.01 \pm 1.12$  mg GAE/g, and  $49.61 \pm 1.30$  mg QE/g, respectively. The graphical representation of responses obtained under the MA-N<sub>A</sub>DESE and HSE processes have been depicted in Figure 5. It could be concluded that a higher extraction yield and antioxidant capacities (DPPH and ABTS), TPC, and TFC can be obtained from orange peel using the MA-N<sub>A</sub>DESE process in comparison to the HSE process. Higher extraction yield, antioxidant capacities (DPPH and ABTS), TPC, and TFC of orange peel may be attributed to high heat efficiency, homogeneous heating, and high speed of microwave radiation over HSE. In addition, N<sub>A</sub>DESE is effective due to its small amount of use, nontoxicity, low flammability, reduced waste generation, negligible vapor pressure, and environmentally friendly behavior. Consequently, MA-N<sub>A</sub>DESE could be employed as a rapid and effective process to extract bioactive substances from orange peel.

#### 4. CONCLUSION AND FUTURE PROSPECTIVES

In this present study, the OFAT approach was adopted to screen the important factors influencing the antioxidant activity of the orange peel. The RSM, ANN techniques, and process parameters were used in this predictive modeling project. The accuracy of the generated model for each response was

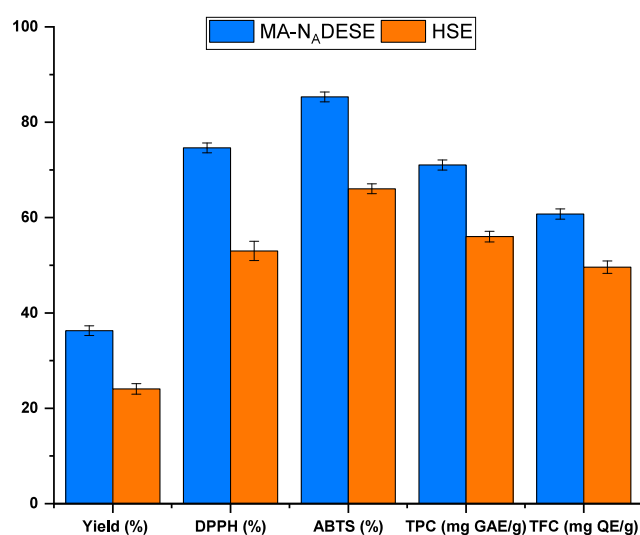


**Figure 5.** Comparison of MA-N<sub>A</sub>DESE and HSE.

accurately anticipated, with a 5% less error rate. For a better prediction of the overall experimental values, the best network topology (4–10–5) and number of neurons to acquire through ANN modeling were both 10. When RSM and ANN modeling for response prediction were compared, it was found that ANN modeling produced better predictions than RSM, as shown by higher coefficient of determination values and lower values for RMSE,  $\chi^2$ , MAE, and AAD%. The MA-N<sub>A</sub>DESE and HSE procedures were compared for higher efficacy and feasibility under optimum conditions, i.e., a rising time of 13 min, 53 °C temperature, a liquid-to-solid ratio of 20 mL/g, and a holding time of 21 min. From the comparative analysis, it can be concluded that MA-N<sub>A</sub>DESE with N<sub>A</sub>DESE-2 (ChCl:EG) at 50% concentration in water was found to be the most effective process over HSE due to the higher extraction

yield and superior antioxidant capacities of the bioactive compounds of orange peel. This study also illustrates the importance of orange peel valorization and the use of sustainable and eco-friendly green extraction techniques for recovery of bioactive compounds with high antioxidant activity, which could find useful applications in the food, pharmaceutical, and cosmetics industries. The effect of other nonconventional techniques such as subcritical, pressurized liquid and their combined effects have to be studied in the future for the extraction of phenolic compounds and could be aimed toward the purification and isolation of these bioactive compounds and whether this process could be exploited on an industrial scale.

## ■ ASSOCIATED CONTENT

### SI Supporting Information

The Supporting Information is available free of charge at <https://pubs.acs.org/doi/10.1021/acsomega.4c04468>.

Figure S1: Response surface 3D plot showing the combined effect of microwave time and temp (a), microwave temp and liquid-to-solid (L/S) ratio (b), temp and holding time (c) on the extraction yield; Figure S2: Response surface 3D plot showing the combined effect of microwave temp and liquid-to-solid ratio (a), microwave temp and holding time (b), liquid-to-solid ratio and holding time (c) on the DPPH; Figure S3: Response surface 3D plot showing the combined effect of microwave temp and liquid-to-solid ratio (a), microwave temp and holding time (b), liquid-to-solid ratio and holding time (c) on the ABTS; Figure S4: Response surface 3D plot showing the combined effect of microwave time and temp (a), microwave temp and liquid-to-solid ratio (b), microwave temp and holding time (c) on the TPC content; Figure S5: Response surface 3D plot showing the combined effect of microwave time and liquid-to-solid ratio (a), microwave temp and holding time (b), liquid-to-solid ratio and holding time (c) on the TFC content; Table S1: Analysis of regression coefficient for all response variables (PDF)

## ■ AUTHOR INFORMATION

### Corresponding Authors

**Anupama Singh** – Department of Food Engineering, National Institute of Food Technology, Entrepreneurship and Management (Institute of National Importance, Under MoFPI, Govt. of India), Kundli, Haryana 131028, India; Email: [asingh3niftem@gmail.com](mailto:asingh3niftem@gmail.com)

**Avvaru Praveen Kumar** – Department of Chemistry, School of Applied Natural Science, Adama Science and Technology University, Adama 1888, Ethiopia; [orcid.org/0000-0001-5012-0666](https://orcid.org/0000-0001-5012-0666); Email: [drkumar.kr@gmail.com](mailto:drkumar.kr@gmail.com)

### Authors

**Rachna Gupta** – Department of Food Engineering, National Institute of Food Technology, Entrepreneurship and Management (Institute of National Importance, Under MoFPI, Govt. of India), Kundli, Haryana 131028, India; School of Biomedical Sciences, Galgotias University, Greater Noida 203201, India

**Prabhat K. Nema** – Department of Food Engineering, National Institute of Food Technology, Entrepreneurship and

Management (Institute of National Importance, Under MoFPI, Govt. of India), Kundli, Haryana 131028, India; [orcid.org/0000-0001-6419-4973](https://orcid.org/0000-0001-6419-4973)

**Tapas Roy** – Department of Food Engineering, National Institute of Food Technology, Entrepreneurship and Management (Institute of National Importance, Under MoFPI, Govt. of India), Kundli, Haryana 131028, India

**Sanjay Kumar** – Department of Food Science and Technology, Graphic Era (Deemed to be University), Dehradun, Uttarakhand 248002, India; Graphic Era Hill University, Dehradun, Uttarakhand 248002, India; [orcid.org/0000-0001-6128-2783](https://orcid.org/0000-0001-6128-2783)

Complete contact information is available at:

<https://pubs.acs.org/10.1021/acsomega.4c04468>

### Author Contributions

R.G.: methodology, formal analysis, and writing original draft. A.S. and P.K.N.: Conceptualization, validation, and supervision. T.R.: formal analysis, review, and editing. S.K.: Formal analysis, validation, review, and editing. A.P.K.: Supervision, review, and editing.

### Notes

The authors declare no competing financial interest.

## ■ ACKNOWLEDGMENTS

The authors are thankful to the Department of Food Science & Technology, Graphic Era (Deemed to be University), Dehradun, Uttarakhand, India, for providing the necessary infrastructure for this research work. The authors are also thankful for the Department of Chemistry, School of Applied Natural Science, Adama Science and Technology University, Ethiopia for necessary support. The authors are grateful to the Ministry of Food Processing Industries (MOFPI), New Delhi, India for granting the financial support; NIFTEM, Sonapat, Haryana, India for the institutional facility.

## ■ REFERENCES

- (1) Panic, M.; Andlar, M.; Tisma, M.; Rezić, T.; Sibalic, D.; Cvjetko Bubalo, M.; Radojčić Redovniković, I. Natural deep eutectic solvent as a unique solvent for valorisation of orange peel waste by the integrated biorefinery approach. *Waste Management* **2021**, *120*, 340–350.
- (2) Panic, M.; Radic Stojković, M.; Kraljić, K.; Skevin, D.; Radojčić Redovniković, I.; Gaurina Srček, V.; Radosević, K. Ready-to-use green polyphenolic extracts from food by-products. *Food Chemistry* **2019**, *283*, 628–636.
- (3) Anticono, M.; Blesa, J.; Frigola, A.; Esteve, M. J. High biological value compounds extraction from citrus waste with non-conventional methods. *Foods* **2020**, *9* (6), 811.
- (4) Chen, X. Q.; Li, Z. H.; Liu, L. L.; Wang, H.; Yang, S. H.; Zhang, J. S.; Zhang, Y. Green extraction using deep eutectic solvents and antioxidant activities of flavonoids from two fruits of *Rubia* species. *Lwt* **2021**, *148*, 111708.
- (5) Manurung, R.; Siregar, A. G. A. Performance of menthol based deep eutectic solvents in the extraction of carotenoids from crude palm oil. *GEOMATE Journal* **2020**, *19* (74), 131–137.
- (6) Abbott, A. P.; Capper, G.; Davies, D. L.; Rasheed, R. K.; Tambyrajah, V. Novel solvent properties of choline chloride/urea mixtures. *Chem. Commun.* **2003**, No. 1, 70–71.
- (7) Reinhardt, D.; Ilgen, F.; Kralisch, D.; König, B.; Kreisel, G. Evaluating the greenness of alternative reaction media. *Green Chem.* **2008**, *10* (11), 1170–1181.
- (8) Nam, M. W.; Zhao, J.; Lee, M. S.; Jeong, J. H.; Lee, J. Enhanced extraction of bioactive natural products using tailor-made deep

- eutectic solvents: application to flavonoid extraction from *Flos sophorae*. *Green Chem.* **2015**, *17* (3), 1718–1727.
- (9) Cvjetko Bubalo, M.; Curko, N.; Tomasevic, M.; Kovacevic Ganic, K.; Radojic Redovnikovic, I. Green extraction of grape skin phenolics by using deep eutectic solvents. *Food Chem.* **2016**, *200*, 159–166.
- (10) Alara, O. R.; Abdurahman, N. H.; Olalere, O. A. Ethanol extraction of flavonoids, phenolics and antioxidants from *Vernonia amygdalina* leaf using two-level factorial design. *Journal of King Saud University-Science* **2020**, *32* (1), 7–16.
- (11) Aung, T.; Kim, S. J.; Eun, J. B. A hybrid RSM-ANN-GA approach on optimization of extraction conditions for bioactive component-rich laver (*Porphyra dentata*) extract. *Food Chem.* **2022**, *366*, 130689.
- (12) Mhatre, M. S.; Siddiqui, F.; Dongre, M.; Thakur, P. A review paper on artificial neural network: a prediction technique. *International Journal of Scientific & Engineering Research* **2015**, *6* (12), 161–163.
- (13) Dai, Y.; Witkamp, G. J.; Verpoorte, R.; Choi, Y. H. Tailoring properties of natural deep eutectic solvents with water to facilitate their applications. *Food Chemistry* **2015**, *187*, 14–19.
- (14) Bosiljkov, T.; Dujmic, F.; Cvjetko Bubalo, M.; Hribar, J.; Vidrih, R.; Brncic, M.; Zlatic, E.; Radojic Redovnikovic, I.; Jokic, S. Natural deep eutectic solvents and ultrasound-assisted extraction: Green approaches for extraction of wine lees anthocyanins. *Food and Bioprocess Technology* **2017**, *102*, 195–203.
- (15) Kumar, M.; Dahuja, A.; Sachdev, A.; Kaur, C.; Varghese, E.; Saha, S.; Sairam, K. V. S. Valorisation of black carrot pomace: Microwave assisted extraction of bioactive phytochemicals and antioxidant activity using Box–Behnken design. *Journal of Food Science and Technology* **2019**, *56*, 995–1007.
- (16) Uysal, S.; Zengin, G.; Aktumsek, A.; Karatas, S. Chemical and biological approaches on nine fruit tree leaves collected from the Mediterranean region of Turkey. *Journal of Functional Foods* **2016**, *22*, 518–532.
- (17) Kumar, S.; Arora, S.; Kumar, V.; Joshi, S.; Naik, B.; Bisht, B.; Tomar, M. S.; Gururani, P. Physicochemical, nutritional, and sensory characteristics of *Chenopodium album*, ashwagandha, flaxseed, and Giloy fortified bun. *Journal of Food Processing and Preservation* **2022**, *46* (12), No. e17265.
- (18) Van Hung, P.; Yen Nhi, N. H.; Ting, L. Y.; Lan Phi, N. T. Chemical composition and biological activities of extracts from pomelo peel by-products under enzyme and ultrasound-assisted extractions. *Journal of Chemistry* **2020**, *2020*, 1–7.
- (19) Kumar, S.; Krishali, V.; Purohit, P.; Saini, I.; Kumar, V.; Singh, S.; Upadhyay, S.; Joshi, H. C.; Wilson, I.; Singh Tomar, M. Physicochemical properties, nutritional and sensory quality of low-fat Ashwagandha and Giloy-fortified sponge cakes during storage. *Journal of Food Processing and Preservation* **2022**, *46* (2), No. e16280.
- (20) Patra, A.; Abdullah, S.; Pradhan, R. C. Application of artificial neural network-genetic algorithm and response surface methodology for optimization of ultrasound-assisted extraction of phenolic compounds from cashew apple bagasse. *Journal of Food Process Engineering* **2021**, *44* (10), No. e13828.
- (21) Cheok, C. Y.; Chin, N. L.; Yusof, Y. A.; Talib, R. A.; Law, C. L. Optimization of total phenolic content extracted from *Garcinia mangostana* Linn. hull using response surface methodology versus artificial neural network. *Industrial crops and products* **2012**, *40*, 247–253.
- (22) Jha, A. K.; Sit, N. Comparison of response surface methodology (RSM) and artificial neural network (ANN) modelling for supercritical fluid extraction of phytochemicals from *Terminalia chebula* pulp and optimization using RSM coupled with desirability function (DF) and genetic algorithm (GA) and ANN with GA. *Industrial Crops and Products* **2021**, *170*, 113769.
- (23) Quan, T.; Wang, D.; Yang, L.; Liu, S.; Tao, Y.; Wang, J.; Deng, L.; Kang, X.; Zhang, K.; Xia, Z.; Gao, D. Effective extraction methods based on hydrophobic deep eutectic solvent coupled with functional molecularly imprinted polymers: Application on quercetin extraction from natural medicine and blood. *Microchemical Journal* **2022**, *174*, 107076.
- (24) Dahmoune, F.; Spigno, G.; Moussi, K.; Remini, H.; Cherbal, A.; Madani, K. Pistacia lentiscus leaves as a source of phenolic compounds: Microwave-assisted extraction optimized and compared with ultrasound-assisted and conventional solvent extraction. *Industrial Crops and Products* **2014**, *61*, 31–40.
- (25) Wang, H.; Ma, X.; Cheng, Q.; Xi, X.; Zhang, L. Deep eutectic solvent-based microwave-assisted extraction of baicalin from *Scutellaria baicalensis* Georgi. *Journal of Chemistry* **2018**, *2018*, 1–10.
- (26) Spigno, G.; De Faveri, D. M. Microwave-assisted extraction of tea phenols: A phenomenological study. *Journal of food engineering* **2009**, *93* (2), 210–217.
- (27) Dobhal, A.; Awasthi, P.; Shahi, N. C.; Kumar, A.; Bisht, B.; Joshi, S.; Kumar, V.; Hussain, A.; Kumar, S. Process optimization of nutritious whey incorporated wheat-barley buns and assessment of their physical, nutritional, and antioxidant profiles. *Journal of Food Measurement and Characterization* **2024**, *18* (3), 1759–1775.
- (28) Handique, J.; Bora, S. J.; Sit, N. Optimization of banana juice extraction using combination of enzymes. *Journal of Food Science and Technology* **2019**, *56*, 3732–3743.
- (29) Mehra, S.; Kandari, A.; Sharma, S.; Kumar, V.; Bisht, B.; Joshi, S.; Tomar, M. S.; Ahmad, W.; Dobhal, A.; Kumar, S. Numerical optimization of microwave heating on bioactive components and quality characteristics of buransh (*Rhododendron arboretum*) flower squash by using response surface methodology (RBD). *Systems Microbiology and Biomanufacturing* **2024**, *4*, 215–222.
- (30) Mohan, S. K.; Viruthagiri, T.; Arunkumar, C. Statistical optimization of process parameters for the production of tannase by *Aspergillus flavus* under submerged fermentation. *3 Biotech* **2014**, *4*, 159–166.
- (31) Alara, O. R.; Abdurahman, N. H.; Ukaegbu, C. I.; Azhari, N. H. *Vernonia cinerea* leaves as the source of phenolic compounds, antioxidants, and anti-diabetic activity using microwave-assisted extraction technique. *Industrial Crops and Products* **2018**, *122*, 533–544.
- (32) Doldolova, K.; Bener, M.; Lalikoğlu, M.; Aşçı, Y. S.; Arat, R.; Apak, R. Optimization and modeling of microwave-assisted extraction of curcumin and antioxidant compounds from turmeric by using natural deep eutectic solvents. *Food Chem.* **2021**, *353*, 129337.
- (33) Wang, Y.; You, J.; Yu, Y.; Qu, C.; Zhang, H.; Ding, L.; Zhang, H.; Li, X. Analysis of ginsenosides in *Panax ginseng* in high pressure microwave-assisted extraction. *Food Chem.* **2008**, *110* (1), 161–167.
- (34) Chen, F.; Xu, M.; Yang, X.; Liu, J.; Xiao, Y.; Yang, L. An improved approach for the isolation of essential oil from the leaves of *Cinnamomum longepaniculatum* using microwave-assisted hydro-distillation concatenated double-column liquid-liquid extraction. *Sep. Purif. Technol.* **2018**, *195*, 110–120.
- (35) Doulabi, M.; Golmakani, M. T.; Ansari, S. Evaluation and optimization of microwave-assisted extraction of bioactive compounds from eggplant peel by-product. *Journal of Food Processing and Preservation* **2020**, *44* (11), No. e14853.
- (36) Rahmani, Z.; Khodaiyan, F.; Kazemi, M.; Sharifan, A. Optimization of microwave-assisted extraction and structural characterization of pectin from sweet lemon peel. *Int. J. Biol. Macromol.* **2020**, *147*, 1107–1115.
- (37) Hayat, K.; Zhang, X.; Chen, H.; Xia, S.; Jia, C.; Zhong, F. Liberation and separation of phenolic compounds from citrus mandarin peels by microwave heating and its effect on antioxidant activity. *Sep. Purif. Technol.* **2010**, *73* (3), 371–376.
- (38) Kumar, S.; Jain, I.; Khare, A.; Kumar, V.; Singh, S.; Gautam, P.; Upadhyay, S.; Anand, J.; Singh, A.; Goswami, U. Numerical optimization of microwave treatment and impact of storage period on bioactive components of cumin, black pepper and mustard oil incorporated coriander leave paste. *Journal of Food Measurement and Characterization* **2022**, *16* (3), 2071–2085.
- (39) Rodsamran, P.; Sothornvit, R. Extraction of phenolic compounds from lime peel waste using ultrasonic-assisted and microwave-assisted extractions. *Food bioscience* **2019**, *28*, 66–73.

(40) Bhuyan, D. J.; Van Vuong, Q.; Chalmers, A. C.; van Alena, I. A.; Bowyer, M. C.; Scarlett, C. J. Microwave-assisted extraction of *Eucalyptus robusta* leaf for the optimal yield of total phenolic compounds. *Industrial Crops and Products* **2015**, *69*, 290–299.

(41) Dorta, E.; Lobo, M. G.; Gonzalez, M. Reutilization of mango byproducts: study of the effect of extraction solvent and temperature on their antioxidant properties. *J. Food Sci.* **2012**, *77* (1), C80–C88.

(42) Kumar, S.; Singh, I.; Kohli, D.; Joshi, J.; Mishra, R. Waste pomelo (*Citrus maxima*) peels—a natural source of antioxidant and its utilization in peanut oil for suppressing the development of rancidity. *Current Research in Nutrition and Food Science Journal* **2019**, *7* (3), 800–806.

(43) Ghafoor, K.; Choi, Y. H.; Jeon, J. Y.; Jo, I. H. Optimization of ultrasound-assisted extraction of phenolic compounds, antioxidants, and anthocyanins from grape (*Vitis vinifera*) seeds. *Journal of agricultural and food chemistry* **2009**, *57* (11), 4988–4994.

(44) Xiao, W.; Han, L.; Shi, B. Microwave-assisted extraction of flavonoids from *Radix Astragali*. *Sep. Purif. Technol.* **2008**, *62* (3), 614–618.

(45) Baş, D.; Boyacı, İ. H. Modeling and optimization I: Usability of response surface methodology. *Journal of food engineering* **2007**, *78* (3), 836–845.

(46) Elnjikkal Jerome, R.; Dwivedi, M. Microwave vacuum drying of pomegranate peel: Evaluation of specific energy consumption and quality attributes by response surface methodology and artificial neural network. *Journal of Food Processing and Preservation* **2022**, *46* (3), No. e16325.